Research Article

Journal of RAMAN SPECTROSCOPY

Received: 8 April 2011 Revised: 10 May 2011 Accepted: 11 May 2011 Published online in Wiley Online Library: 1 July 2011

(wileyonlinelibrary.com) DOI 10.1002/jrs.3012

Conformational polymorphism of the antidiabetic drug chlorpropamide

A. P. Ayala,[a,b]* M. W. C. Caetano,[a] S. B. Honorato,[a] J. Mendes Filho,[a] H. W. Siesler,[c] S. N. Faudone,[d] S. L. Cuffini,[d] F. T. Martins,[b] C. C. P. da Silva,[b] and J. Ellena[b]

In this paper, the main features of Raman spectroscopy, one of the first choice methods in the study of polymorphism in pharmaceuticals, are presented taking chlorpropamide as a case of study. The antidiabetic drug chlorpropamide (1-[4-chlorobenzenesulphonyl]-3-propyl urea), which belongs to the sulfonylurea class, is known to exhibit, at least, six polymorphic phases. These forms are characterized not only by variations in their molecular packing but also in their molecular conformation. In this study, the polymorphism of chlorpropamide is discussed on the basis of Raman scattering measurements and quantum mechanical calculations. The main spectroscopic features that fingerprint the crystalline forms are correlated with the corresponding crystalline structures. Using a theoretical approach on the energy dependence of the conformers, simulated molecular torsion angles are plotted *versus* the formation energy, which provides a satisfactory agreement between the torsion angles at the energy minima and the experimental values observed in the different solid forms of chlorpropamide.

Keywords: chlorpropamide; polymorphism; Raman spectroscopy; DFT

Introduction

Polymorphism is an important branch in the supramolecular chemistry of the solid state, having special significance in the context of pigments and pharmaceutical substances.[1] This phenomenon is defined as the ability of a compound to crystallize in different crystalline phases with different arrangements and/or conformations of the molecules in the crystal lattice.[2–4] The importance of polymorphism in pharmaceuticals has been widely documented. Polymorphs of active pharmaceutical ingredients (APIs) can differ in their chemical and physical properties, including melting point, chemical reactivity, apparent solubility, dissolution rate, optical and mechanical properties, vapor pressure, and density. The polymorphs of a drug may exhibit different solubilities and dissolution rates, which, particularly if the compound possesses poor solubility, may result in variable absorption and bioavailability problems. As a result, polymorphism can affect the quality, safety, and efficacy of a drug product.[5–7]

Vibrational spectroscopy methods are well-established tools for the characterization of APIs in the solid state. Focusing on the study of the fundamental vibrational modes, these methods comprise infrared absorption (far and mid), terahertz pulsed spectroscopy, and Raman scattering. During the last 20 years, the use of Raman spectroscopy in the study of pharmaceutical compounds has been growing exponentially. A detailed analysis of the literature in this field reveals that the increased interest in Raman scattering in this field started in the early 1990s, coinciding with the launch of the first Fourier transform (FT) Raman spectrometer. On the other hand, dispersive spectrometers also benefited with the advent of modern instrumentation, which has drastically reduced the cost of the equipment allowing the use of this technique for routine analytical applications. Nowadays, Raman spectroscopy is one of the first choice methods in the study of polymorphism in pharmaceuticals. Several reviews have discussed the advantages and disadvantages of the different vibrational methods.[8–13] However, in this study the main features of Raman spectroscopy will be presented, taking chlorpropamide, a well-established polymorphic compound, as a case of study.

Therapy with sulfonylurea drugs was instituted in type II diabetic patients at the beginning of the 1950s. Chlorpropamide (Diabinese), 4-chloro-*N*-(propylamino-carbonyl)benzenesulfonamide ($C_{10}H_{13}ClN_2O_3S$, Fig. 1), is a sulfonylurea derivative presenting prolonged pharmacological action.[14] Chlorpropamide belongs to Class II of the biopharmaceutical classification exhibiting poor solubility, which causes problems during absorption. The polymorphic character of chlorpropamide was first reported by Simmons,[15] but Burger[16,17] performed a careful screening of the crystalline forms, identifying five polymorphs. These forms exhibit very complex thermodynamic relationships involving temperature, pressure, and kinetics-induced phase transformations. Calorimetric studies have shown that the phase stability is highly dependent of the

* *Correspondence to: A. P. Ayala, Department of Physics, Federal University of Ceará, PO Box 6030, 60455-970 Fortaleza, CE, Brazil. E-mail: ayala@fisica.ufc.br*

a *Depertamento de Física, Universodade Federal do Ceará, 60455-970 Fortaleza, CE, Brazil*

b *Instituto de Física de São Carlos, University of São Paulo, 13560-970 São Carlos, SP, Brazil*

c *Department of Physical Chemistry, University of Duisburg-Essen, Essen D45117, Germany*

d *CEPROCOR-Ministerio de Ciencia y Tecnologia de Córdoba. CONICET, Argentina; Dept of Pharmaceutical Sciences. Federal University of Santa Catarina, CEP: 88040-900 Florianópolis, SC, Brazil*

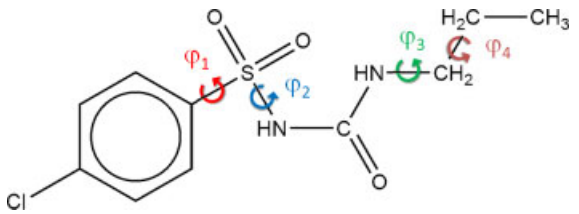

Figure 1. Scheme of the chlorpropamide molecule with φ_1, φ_2, φ_3, and φ_4 indicating selected torsion angles.

thermal history of the sample,[16,18] giving rise to metastable forms that transform into the most stable form through temperature- or time-dependent processes. Furthermore, chlorpropamide has been considered a model compound that exhibits a polymorphic transition under compression during tableting,[5,19,20] although the detailed mechanism of this pressure-induced process has not been not fully elucidated.[19,21–26]

Despite the fact that chlorpropamide polymorphism is well known, there is no standardized nomenclature to refer to these forms. Vemavarapu *et al*.[27] reviewed the literature in this field and correlated the most commonly used nomenclatures, increasing the number of reported polymorphs to seven. In this study, we will follow the notation established by Burger in his former publication. According to the Burger's nomenclature, the polymorphs are labeled I, II, III, IV, and V, with form III being the commercial one. At this point, it is worthwhile to cite that forms I, II, and III are usually referred to as C, B, and A, respectively, due to the wide diffusion of the nomenclature defined by Simmons *et al*.[15] Recently, Debrushchak *et al*. proposed a new notation based on the order in which the crystal structures were elucidated. The proposed nomenclature uses Greek characters as follows: α (III), β (II), γ (IV), δ (VI), and ε (I).[28–32] A transition from the polymorph ε (I) to a new form ε' (I′) at low temperatures was observed by Debrushchak *et al*.[29] using X-ray diffraction and infrared spectroscopy, and by Pérez *et al*. using nuclear quadrupolar resonance (NQR) spectroscopy.[33]

The solid forms of chlorpropamide were traditionally characterized by X-ray powder diffraction,[5,15,18,19,23,24,25,27,34–36] differential scanning calorimetry,[15,16,18,23,35,37] vibrational spectroscopy,[8,15,37–39] and NQR.[33] From the point of view of the use of vibrational spectroscopy, Al-Saieq and Riley[34] reported the infrared absorption spectra of the five solid forms. On the other hand, Tudor *et al*.[39] used FT-Raman spectroscopy to quantify mixtures of forms III and II. Wildfong *et al*. monitored the pressure-induced transformation from form III to form I through *in situ* Raman spectroscopy.[23] Recently, Chesalov *et al*. presented the FT-Raman and FT-IR spectra of five polymorphs, comparing them with *ab initio* calculations.[36]

In this paper, the conformational polymorphism of chlorpropamide is discussed on the basis of the available structural data, Raman spectroscopy, and quantum mechanical calculations. The experimental data are correlated with a conformational scan of the energy landscape performed through quantum mechanical calculations. These results allowed us to identify the energetic relationships between the polymorphs. Thus, the geometrical, conformational, and spectroscopic features are compared among the described polymorphic forms in order to point out some important differences between them, which could give in-depth information of the structure–property relationships of chlorpropamide solid-state forms.

Experimental

Chlorpropamide (form III, Unifarma, Argentina) and the hexanol solvent (analytical grade) were used as raw materials. Preparation methods for chlorpropamide polymorphs were based on the procedure previously reported[15,16,28,36] and summarized here:

1. Form I: the raw material was heated at 110 °C during 1 h and cooled down to room temperature.
2. Form II: the raw material was melted at 110 °C and then the cooling was controlled to 0.1 °C/min down to room temperature.
3. Form III: commercial raw material.
4. Form IV: the raw material was dissolved until a saturated solution in hexanol was obtained at 60 °C. The solution was filtered and cooled to −10 °C. The crystals were dried under vacuum.

The samples were characterized by powder X-ray diffraction and differential scanning calorimetry in order to identify the corresponding crystalline form. FT-Raman spectra were recorded from the original samples on a Bruker IFS55 FT-IR/FT-Raman spectrometer equipped with an Nd : YAG laser (1064 nm excitation line) and a liquid-nitrogen-cooled Ge detector. FT-Raman spectra were acquired by accumulating 1024 scans at a spectral resolution of 4 cm^{-1}. Dispersive Raman spectra were measured using a Jobin Yvon T6400 subtractive triple spectrometer equipped with a liquid-nitrogen-cooled charge coupled device (CCD) detector and exiting the sample with the 514.5 nm line of an Ar laser.

To relate the conformational features of the polymorphs with their crystal packing patterns, Hirshfeld surfaces were calculated for the forms I, II, III, IV, and VI of chlorpropamide using the program Crystal Explorer.[40] The two-dimensional fingerprint plots allow the easy identification of characteristic interactions throughout the structures. Briefly, such fingerprint plots are graphics of d_e (external distance, defined as the separation between the Hirshfeld surface and the nearest atom of an adjacent molecule within the crystal) *versus* d_i (internal distance, defined as the shortest separation from the Hirshfeld surface to an atom nucleus within the same molecule). The parameter d_i gives an idea of the atomic and ionic sizes, whereas d_e states on short intermolecular contacts, and, therefore, they are the key to interpreting the relationships between the intramolecular and intermolecular details by establishing the interplay of the crystal packing with the molecular conformation. Fingerprints are plotted in the range of *d*-values between 0.4 and 2.6 Å with a color gradient from blue to red according to the fractional contribution of the each pair in respect of the overall Hirshfeld surface, where the blue color represents lowered proportions, green is an intermediary contribution, and red implies in an upper limit fraction of 0.1% or greater to the total surface area.

The conformational landscape of chlorpropamide was explored through a systematic variation of four dihedral angles (Fig. 1). The electronic structure and optimized geometry were computed within the density functional theory using Gaussian 03,[41] employing a hybrid of Becke's nonlocal three-parameter exchange functional and the Lee–Yang–Parr correlation functional (B3LYP).[42–44] Rotational energy profiles around the torsion angles were determined by using the 3-21G* basis set. The energy was calculated at 10° intervals of the dihedral angle between −180° and 180°. Rotational energy profiles were calculated by freezing one torsion and relaxing the remaining parameters (bond angles, bond lengths, and dihedral angles), which were optimized

Journal of RAMAN SPECTROSCOPY

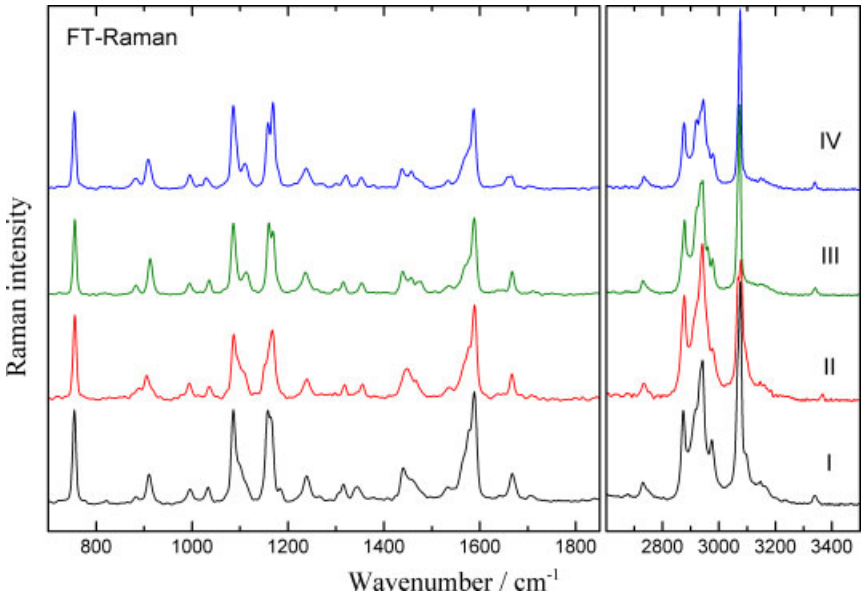

Figure 2. FT-Raman scattering spectra of the polymorphs of chlorpropamide.

in the previous step of the relaxed scan. Raman scattering cross sections were calculated after geometrical optimization using the same functional but the 6–31++G(d,p) basis set. The molecular conformations extracted from the determined crystal structures were used as the starting point. Raman spectra were simulated by convolving the scattering cross section with a Lorentzian profile and considering the thermal distribution of the vibrational modes.[45,46] Potential energy distributions (PEDs) along internal coordinates were calculated by the software Gar2ped.[47] The internal coordinate system recommended by Pulay *et al*.[48] was used for the assignment of vibrational modes.

Results and Discussion

The sensitivity of the Raman scattering spectroscopy to detect structural changes makes it one of the first choice methods in the study of the solid forms of drugs, that is, polymorphs, solvates, hydrates, salts, co-crystals, etc. The most frequent application in pharmaceutical solids is based on the use of this technique in the production of fingerprints of the crystal forms of interest.[49–54] Thus, we will start our discussion by presenting the spectral fingerprints of the polymorphs of chlorpropamide. The FT-Raman spectra of the crystalline forms of chlorpropamide investigated in this study are presented in Fig. 2. In general, our results are in good agreement with the previously reported Raman spectra.[36,39]

The higher wavenumber fundamental vibrations of chlorpropamide are the ν(NH) stretching modes. These bands are observed at 3339 cm^{-1} in forms I, III, and IV, but are shifted toward higher wavenumbers in forms II (3367 cm^{-1}) and VI (3346 cm^{-1}).[36] These modes usually provide information about the crystal packing. The red shift of the ν(NH) stretching modes can be related to the intermolecular hydrogen bond interactions that stabilize the solid forms. This assumption is supported by the reported crystal structures, where NH is bonded to the sulfonyl and/or carbonyl moieties.[23,28,31,32] Particularly, some acceptor–donor distances of the N–H bonds are slightly larger in forms II and VI featuring weaker hydrogen bond interactions, in good agreement with the smaller red shift observed in these polymorphs. A similar behavior has been observed in the infrared spectra reported by Al-Saieq and Riley[34] and Chesalov *et al*.[36]; the ν(NH) modes clearly fingerprint the forms II and VI, whereas the remaining forms exhibit similar absorption bands.

Below 3200 cm^{-1}, the vibrational spectra exhibit two groups corresponding to the ν(CH) stretching modes. The first group, around 3070 cm^{-1}, originates from the ν(CH) of the benzene ring, whereas between 2800 and 3000 cm^{-1} the symmetric and antisymmetric ν(CH) stretching modes belonging to the methyl and methylene groups are superimposed. Our results are in good agreement with the Raman spectra of forms II and III reported by Tudor *et al*.[37,39] These authors were able to discriminate forms II and III using the ν(CH) stretching modes belonging to the aliphatic moieties. This effect may be explained by considering that forms II and III mainly differ in the orientation of the alkyl tail, which is responsible for the vibrational modes around 2900 cm^{-1}. Furthermore, two weak hydrogen bonds connecting one of the methylene and the methyl groups with the sulfonyl moiety, characteristic of form III, may also induce the observed changes in the vibrational spectra. Nevertheless, Fig. 2 shows that, by considering the four polymorphs, the differences are not strong enough to allow the univocal assignment of the crystal forms.

Between 1800 and 700 cm^{-1}, the main vibrational modes of the substituted benzene ring can be identified by comparing the Raman spectra of chlorpropamide and 1,4-dichlorobenzene. Thus, the bands at 1587 cm^{-1} correspond to the ν(C═C) stretching modes (8a and 8b in the Wilson's notation[55]), and that observed at 755 cm^{-1} is the in-phase ring bending (6a). Notice that these bands exhibit no dependence on the crystal form. Tudor *et al*. also distinguish between forms II and III using the doublet located around 1100 cm^{-1}, which may be associated with the breathing (1) and the trigonal (12) deformations of the ring. The same authors also pointed out that the δ(CH) deformation bands of the methyl and methylene groups (~1460 cm^{-1}) fingerprint forms II and III. However, in the attempt to generalize this method to the identification of the four polymorphs, one may observe that the classification is again not univocal. One may reach similar conclusions by inspecting the doublet around 1170 cm^{-1},

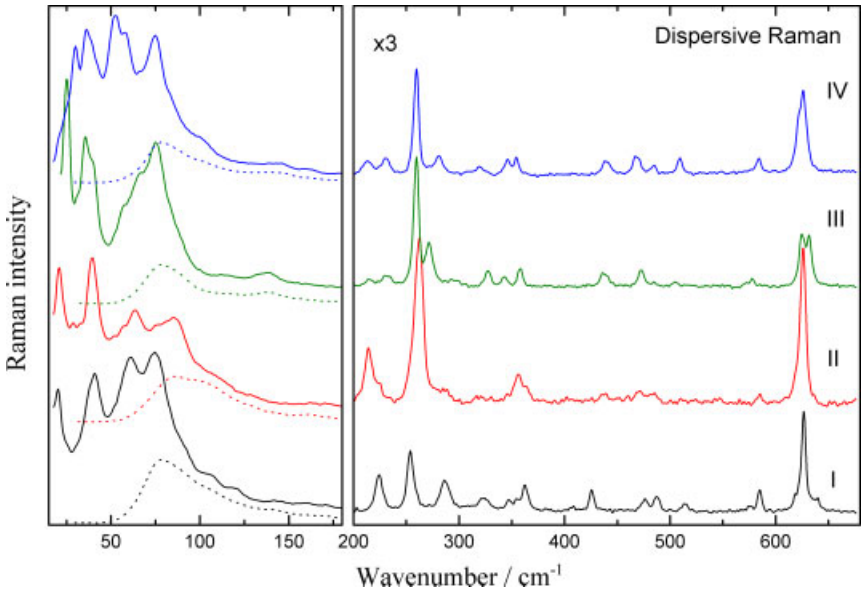

Figure 3. Dispersive Raman scattering spectra of the polymorphs of chlorpropamide. The corresponding FT-Raman spectra (dotted lines) below 200 cm^{-1} are included for comparison.

arising from CH and NH deformations. Carbonyl bands usually reflect the changes in the intermolecular interactions and could be employed for identifying different polymorphs. Instead, in chlorpropamide the ν(C═O) is observed at ~1668 cm^{-1} in forms I to III, at 1658 cm^{-1} in forms IV, and at 1671 cm^{-1} in form VI. In the same spectral region, the sulfonamide group gives rise to bands related to the antisymmetric (triplet between 1280 and 1340 cm^{-1}) and symmetric SO_2 (doublet at 1160 cm^{-1}) stretching modes. Neither the bands associated with the sulfamide group nor the deformations of the alkyl (1400–1500 cm^{-1}) fragments provide distinctive signatures in the Raman spectra identifying unambiguously the crystal forms.

Summarizing, Raman spectra of chlorpropamide above 700 cm^{-1} exhibit only small dependence on the crystal structure. The effects of polymorphism on the vibrational spectra are mostly related to band shifts very close to the instrumental resolution and variations of the relative intensities and line widths. The low sensitivity of Raman spectroscopy in this spectral region suggests that the structural modifications associated with the polymorphs of chlorpropamide could be related to changes in the molecular backbone more than to specific molecular subgroups. This hypothesis is supported by the reported crystal structures. Torsional modes involving the molecular skeleton are expected in the low wavenumber region, which is hardly accessible using conventional infrared absorption spectroscopy. One should also focus attention on intermolecular modes, *i.e.* collective translational or rotational motions of the molecules in the unit cell. These modes produce dynamic deformations of the crystal lattice called lattice vibrations or lattice phonons, whose frequencies, involving Raman shifts in the range (10–150 cm^{-1}), probe the intermolecular interactions and are hence very sensitive to the molecular packing. Even though Raman spectroscopy may extend the spectral range usually observed by IR, the devices used to reject the excitation line, like Notch filters, impose a low-energy cutoff of approximately 80 cm^{-1}, limiting the spectral range of FT and simple dispersive spectrometers. On the other hand, a triple spectrometer working in the subtractive mode provides an excellent rejection of the excitation line, allowing the reduction of the lower spectral limit down to few wavenumbers.[8] The extended spectral range allows the observation of the lattice and skeleton vibrational modes. The relationship between each lattice phonon pattern (lattice dynamics) and its corresponding X-ray diffraction pattern (lattice structure) makes Raman spectroscopy a powerful tool in the identification of the polymorphic forms of pharmaceutical compounds.

Fig. 3 shows the low wavenumber region of the dispersive Raman spectra of the polymorphs of chlorpropamide investigated in this work. Below 700 cm^{-1}, several features fingerprinting the solid forms are identified in these spectra. Between 200 and 700 cm^{-1}, the most significant bands are those around 630 and 260 cm^{-1}. The main band of the first region, which may receive contributions from the in-plane deformation of the aromatic ring and the SO_2 group, splits in forms III and IV, and exhibits some side bands in form I. The second region, determined by deformations of the molecular skeleton and the libration of the methyl group, is especially interesting for the visual identification of the polymorphs. Thus, between 300 and 200 cm^{-1}, changes are observed not only in the number of bands (three, two, four, and four bands are observed in polymorphs I, II, III and IV, respectively) but also in their relative wavenumbers. Finally, the region below 200 cm^{-1} needs to be considered separately, since in it lie most of the torsion vibrations as well as the lattice modes. In this figure, the corresponding FT-Raman spectra were included, for comparison, as dotted lines. Notice that the experimental limitations of the interferometric method completely disguise the low wavenumber modes. Conversely, dispersive Raman spectra of the investigated solid forms are clearly different, providing signatures for their discrimination. This spectral range supplies a very sensitive tool to distinguish among the crystal forms since, regardless of the conformational changes in the molecule, the definition of polymorphism suggests that the crystal lattice, as well as the vibrational modes associated with it, should change from one polymorph to another. Unfortunately, it is not possible to perform an assignment of the low energy bands by direct comparison with other molecules. However, the improvement of the quantum mechanical calculation methods combined with the

Journal of RAMAN SPECTROSCOPY

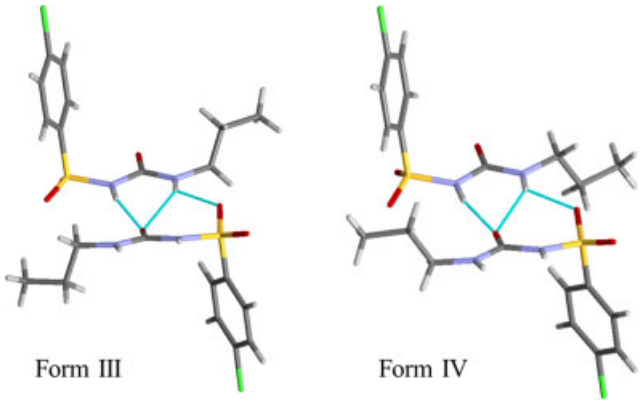

Figure 4. Molecular conformation and intermolecular hydrogen bonds of the polymorphs III and IV of chlorpropamide.

development of faster hardware has made the simulation suitable for the vibrational spectrum of complex molecules.[46,51,56–58]

In order to understand the origin of the conformational polymorphism of chlorpropamide, at this point, it is worthwhile to review the main structural features of the crystal forms. The crystal structure of the most stable polymorph (form III) was reported for the first time in 1980.[28] It crystallizes in an orthorhombic non-centrosymmetric space group $P2_12_12_1$ with four molecules per unit cell. Recently, the polymorphism of chlorpropamide received renewed attention and several crystal structures have been determined. Drebushchak *et al*. have published the molecular structure of two conformational polymorphs, belonging to the centrosymmetric orthorhombic space group *Pbcn* (form II) and the non-centrosymmetric monoclinic one $P2_1$ (form IV).[31,32] The structure of form I was determined from single-crystal[18] and powder diffraction data.[23] The existence of a new polymorph of chlorpropamide was proposed by Drebushchak *et al*. based on thermal analysis, vibrational spectroscopy, and X-ray powder diffraction.[18,36] These experimental data clearly fingerprint a new crystal structure, which has been classified as δ,[18,36] but, based on the original Burger's notation,[16] it could be labeled as form VI. Form VI was proposed to be centrosymmetric orthorhombic belonging to the *Pbcn* space group and exhibiting an uneven molecular conformation.[18]

Two representative conformers of chlorpropamide are presented in Fig. 4. The analysis of the intermolecular interaction pattern that keep stable the three-dimensional network of the five structurally characterized polymorphs of chlorpropamide shows that they present approximately the same crystal packing (Fig. 4). As a rule, the carbonyl group forms a bifurcated intermolecular hydrogen bond with the two amine hydrogen atoms, whereas the SO_2 oxygen atom, *cis* to the carbonyl moiety, accepts the hydrogen from the nitrogen which is covalently bonded to the methylene carbon of the *n*-propyl side chain. Such intermolecular interactions align the sulfonylurea moieties in a plane of alternating chlorpropamide molecules, leading to the formation of one-dimensional chains along one of the crystallographic axes. The alternate stacking of the chlorpropamide molecules favors the formation of the NH···O=C hydrogen bonds (Fig. 4). In addition to the classical intermolecular contacts reported for all polymorphs, there are other weak intermolecular interactions of the C–H···O=S type, which seem to play a decisive role in the conformational features of the conformers.

The main difference between the reported crystalline forms lies in the conformation of the asymmetric unit formed by a single chlorpropamide molecule. Two kind of conformational modifications can be identified. Taking as a reference the sulfonylurea moiety, the reported polymorphs may be differentiated on the basis of the relative orientation of the aromatic ring and the alkyl tail. Related to the *n*-propyl fragment, forms II and IV present the methyl and intermediate methylene groups in the *cis* position to the benzene ring, whereas in forms III and VI the ethyl group is in the *trans* position to the phenyl head. Therefore, the unique, notable structural dissimilarity between the conformers III and VI is in the axially oriented ethyl moiety of the form VI. Concerning the spatial orientation of the cyclic head, the forms III, IV, and VI exhibit approximately the same relative conformation of the phenyl ring. Nevertheless, in forms I and II the phenyl dihedral angles are considerably different from that of the other polymorphs. In addition, these forms are marked by a significant twist on the S–C bond, which alters the values of torsion angles involving the cyclic system and the neighboring sulfonyl group.

Important observations concerning chlorpropamide polymorphs were possible by analyzing the fingerprint plots derived from Hirshfeld surfaces, which were generated by assembling the (d_i, d_e) pairs defined on each individual spot of the calculated surface into the two-dimensional grids.[40] The obtained graphics are very useful for viewing the chemical environment at a specific point of any molecule within the crystal. In Fig. 5, the two-dimensional fingerprint plots of chlorpropamide forms I, II, III, IV, and VI represent the intermolecular contact schemes for these polymorphs. The Hirshfeld surface of the most stable polymorph, i.e. form III, was also included in order to emphasize the most relevant features of the fingerprint plots. All plots are featured by the presence of sharp spikes (υ) that can be related with the strong NH···O=C and NH···O=S hydrogen bonds responsible by the alignment of the sulfonylurea cores onto a plane where the chlorpropamide molecules are alternated. As previously discussed, these contacts lead to the formation of one-dimensional chains which are reported for all the polymorphs used in the Hirshfeld surface construction. A remarkable difference among the fingerprint plots for the chlorpropamide polymorphs can be pointed out by examining the regions containing the short H···N (ϖ), H···Cl (ω), and H···H (ξ). The first two sets of short distances are mainly related to the packing of the previously described chains. The H···N and H···Cl distances characterize the packing in the directions perpendicular and parallel to the plane defined by the sulfonylurea groups of the chain. On the other hand, the shorter H···H are ascribed to the neighbor of the alkyl tail, being directly related to the molecular conformation. In the case the chlorpropamide form VI, the short H···H contact region is strongly split, which cannot be seen in the fingerprint graphics for the all other forms. Such splitting is at $d_i \approx d_e \approx 1.21$ Å and it is due to the presence of a closed H···H contact involving three atoms in opposition to one where just two atoms are directly connected. Specifically, this contact involves a hydrogen atom of the phenyl ring, another one of the methylene group of the aliphatic branch, and one of the hydrogen atoms of the methyl group within the propyl side chain. In this way, the fingerprint plots derived from the Hirshfeld surfaces for the chlorpropamide polymorphs emphasize the differences between the corresponding crystal packing of these forms. Mainly, the splitting at the area of the short H···H contacts, which is a consequence of H···H intermolecular contacts between the aromatic head and the propyl branch, has revealed that the axial orientation of the ethyl moiety in relation to the

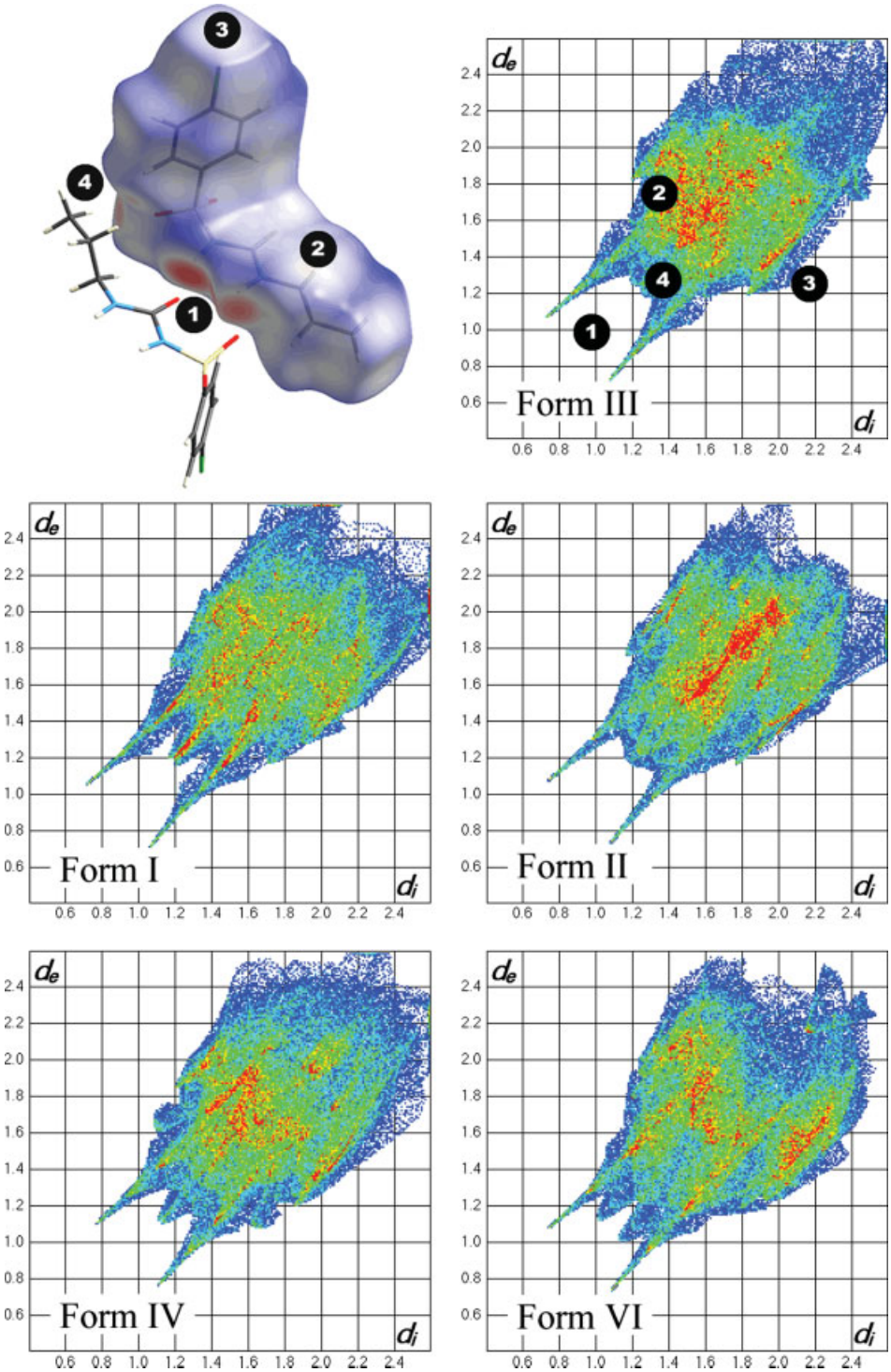

Figure 5. Two-dimensional fingerprint plots for the chlorpropamide polymorphs. Color gradation: the low frequency of occurrence of a (d_i, d_e) pair is represented by blue, and green corresponds to an intermediary contribution to the total Hirshfeld surface area. Red color would imply in a high frequency of the surface points with the same (d_i, d_e) association.

sulfonylurea plane and its *trans* configuration to the substituted phenyl group are driving certain hydrogen atoms of the aliphatic and aromatic portions to get close within the crystal structure.

Hirshfeld surfaces and the corresponding fingerprints can be correlated with the vibrational spectra since both are mainly determined by the chemical environment of the molecule. These results emphasize the relevance of the alkyl tail in the conformational polymorphism of chlorpropamide, as reflected by the vibrational modes related to this moiety. However, the key parameters that describe doubtlessly the different conformers are the torsion angles of the molecular backbone. The six most relevant torsion angles of chlorpropamide polymorphs are compared in Table 1. Considering the experimental evidences, the torsion angles S–N–C–N and N–C–N–C are not interesting for our

Journal of RAMAN SPECTROSCOPY

Table 1. Backbone torsion angles of the chlorpropamide polymorphs

Form	CCSN (φ_1)	CSNC (φ_2)	SNCN	NCNC	CNCC (φ_3)	NCCC (φ_4)
I (ε)	130.48	−47.60	145.48	174.72	93.61	−179.35
II (β)	105.16	−62.97	168.79	178.59	94.55	179.72
III (α)	82.24	−76.20	170.22	175.30	−104.16	−176.05
IV (γ)	86.35	−72.10	173.22	−179.34	87.54	−177.17
VI (δ)	79.06	−76.55	168.07	179.42	−121.05	57.78
I′ (ε')	83.48	−74.92	168.84	178.99	−100.42	−174.73

discussion, since they transform the urea group from a *cis* to a *trans* configuration, which was not observed experimentally. The notation to be used is indicated in Fig. 1. On one side of the chlorpropamide molecule, the orientation of the phenyl ring is described by φ_1, whereas φ_2 relates the conformation of the sulfonylurea group. On the other side, either up or down orientation and the conformation of the alkyl tail are stated by φ_3 and φ_4, respectively.

Quantum mechanical calculations of the energy surface of the free molecule were also employed to explore the relationship between the formation energy spent on theoretical chlorpropamide torsion angles and the observed conformational details. The angular dependence of the relative formation energies is plotted in the Fig. 6, where the experimental values for the different polymorphs are indicated by arrows. In the most stable forms (III and IV), φ_1 lies around the energy minimum, whereas in forms I and II, this torsion is at unstable places. The two minima observed in Fig. 6(a) correspond to the 180° rotation of the phenyl ring, which produces equivalent conformations. It is important to note that the form I is at an inflexion point, which provably has been transformed in a metastable minimum by the intermolecular interactions. Furthermore, various experimental evidences show that forms I and II easily transform to form III. This process could be associated with the off-equilibrium conformation of these forms. There is little dependence of the experimental conformations on the φ_2 torsion. The φ_2 angular dependence of the energy (Fig. 6(b)) exhibits two stable points at ±90°, which are associated with the up and down configurations of the aromatic ring perpendicular to the sulfonylurea group. Nevertheless, this last orthogonal conformation has not yet been observed experimentally. The orientation of the alkyl ring is depicted by φ_3 (Fig. 6(c)). Two flat minima separated by a smaller potential barrier (placed at 180°) characterize the energy dependence on φ_3. This result is in an excellent agreement with the experimental observations, since they clearly describe either up or down orientations of the alkyl tail. Furthermore, the trend of the forms I, II, and IV to convert into form III is supported by the low potential barrier relating them, which could be also be stated of the polymorph VI. Finally, three minima with similar energies are available for φ_4 (Fig. 6(d)). Since all the early reported crystal forms exhibit an equatorially oriented ethyl tail, the forms I, II, III, and IV present practically the same conformation with the N–C–C–C twist measurement near ±180°. So, the observed φ_4 torsion angles of these four polymorphs are at one of the energy minima. Thus, those structures suggested that the key torsion in the conformational polymorphism of chlorpropamide is φ_3, which determines the relative orientation of the phenyl ring and the alkyl tail. The remaining dihedral angles were around well-defined specific minima providing minor corrections to the molecular conformation. Interestingly, the

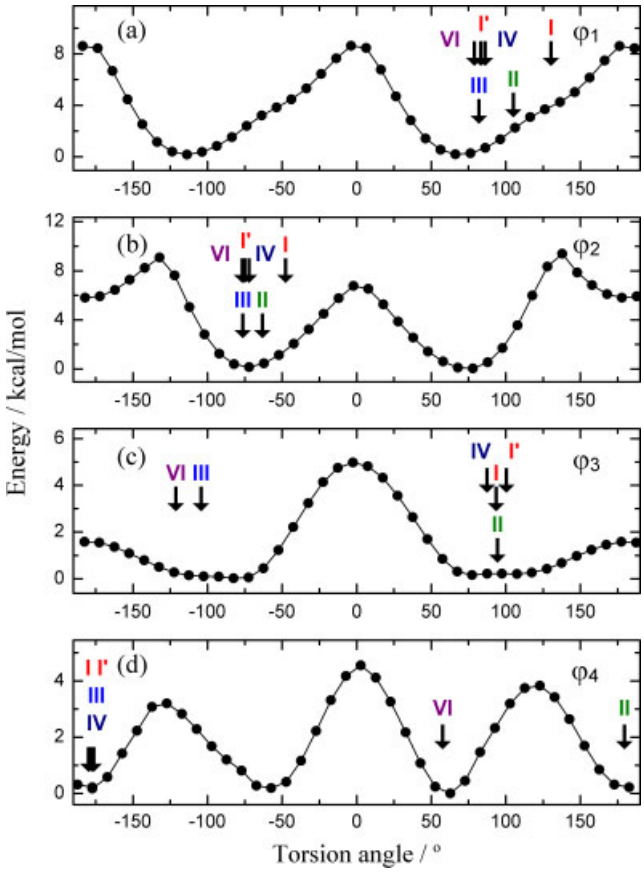

Figure 6. Energy scanning of the (a) φ_1, (b) φ_2, (c) φ_3 and (d) φ_4 torsion angles of the chlorpropamide molecule. Arrows indicate the experimentally determined values from the crystalline structure of the chlorpropamide polymorphs.

polymorph VI evidenced the relevance of the φ_4 angle, which is at another energetic minimum close to 57°, corresponding to the axial position of the *trans*-oriented ethyl moiety. In conclusion, the quantum mechanical exploration of the conformational energy landscape of chlorpropamide has precisely described all the observed molecular conformations, and a further chlorpropamide polymorph at least remains without structure characterization, since the crystal form with the experimental φ_4 value at the third energetic ground (approximately −57°) can be predicted as a *cis* and axially configured ethyl tail polymorph.

The analysis of the crystal structures evidenced that the skeleton torsions play a key role in the conformational polymorphism of chlorpropamide. Furthermore, vibrational modes associated with these dihedral angles are expected at low wavenumbers. The strong dependence of the Raman spectra below 200 cm^{-1} supports this hypothesis, but quantum mechanical calculations could shed some light on this problem. Chesalov *et al*. have calculated the vibrational modes of three conformers above 200 cm^{-1}.[36] In Fig. 7, the experimental and calculated Raman spectra below 200 cm^{-1} of the forms III and IV are presented. These conformers were selected because they are representative of the most relevant features of the conformational polymorphism of chlorpropamide. In addition, Table 2 lists the experimental and calculated low energy modes together with the corresponding PEDs. Especially in the case of form IV, there is a good agreement between the calculation and the experimental result. This is

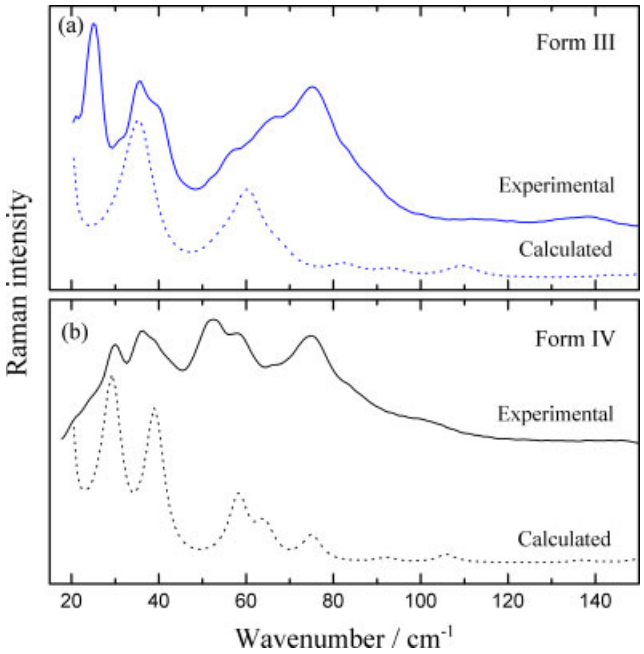

Figure 7. Experimental and calculated Raman spectra of the polymorphs (a) III and (b) IV of chlorpropamide.

because the optimized geometry of the conformer IV is closer to the experimental one than that of form III. A one-to-one assignment was performed, showing that the two low energy modes seem to be related to lattice vibrations. The PED distribution confirms that the remaining modes originate from torsions of the molecular skeleton.

Since Raman scattering measurement can be easily performed under extreme conditions (temperature, pressure, moisture, etc.), this experimental method is particularly suitable to investigate structural transformations in APIs, such as polymorphic transitions and solvatation/desolvatation processes.[59–62] In the case of chlorpropamide, we have investigated the solid–solid phase transformation exhibited by form I. At low temperature, this polymorph transforms into a new phase, labeled as ε' by Drebushchak *et al.* (I′ in our notation), but the critical temperature differs depending on the experimental method used to probe the transition. IR and X-ray powder diffraction measurements evidenced the appearance of the new phase between −150 and −10 °C depending on the thermal history of the sample.[29] Both methods clearly show the coexistence of forms I and I′ down to −190 °C. The same transformation was observed by NQR at −85 °C as a very sharp transition without evidences of phase coexistence.[33] It is interesting to notice that the forms I′(ε') and III have approximately the same molecular conformation (Table 1), differing only in the molecular packing.

Fig. 8(a) and (b) shows the temperature dependence of the FT-Raman spectra of form I of chlorpropamide. As a rule, the recorded spectra change continuously as the temperature is brought down. However, a detailed analysis of the data allowed us to identify anomalous behaviors around 260 and 2900 cm^{-1}. The phase transformation is evidenced by the splitting of the bands at 255 and 2870 cm^{-1}, which mainly originate from the C–X out of plane deformation of the *p*-benzene moiety and CH stretchings of the alkyl tail, respectively. Since the phase transition is driven by the reorientation of the phenyl ring and the alkyl tail, the spectroscopic

Table 2. Selected scaled DFT and experimental Raman fundamental vibrational modes[a] (in cm^{-1}) of forms III and IV of chlorpropamide

DFT	Experimental	PED[b] (%)
Form III		
	25	Lattice
	31	Lattice
35	35	$\tau[\varphi_2](62) + \tau$[SNCN](62)
52	40	τ[SNCN](39) + $\tau[\varphi_3](53)$
59	56	$\tau[\varphi_1](59) + \tau$[SNCN](31)
67	66	$\tau[\varphi_2](11) + \tau$[NCNC](62)
82	75	Ph[*11b*](12) + $\tau[\varphi_1](15) + \tau$[SNCN](45) + $\tau[\varphi_4](15)$
91	86	τ[SNCN](26) + τ [NCNC](14) + $\tau[\varphi_3](28)$ + $\tau[\varphi_4](20)$
108	115	$\tau[\varphi_2](61) + \tau$[NCNC](21)
140	137	$\tau[\varphi_2](22) + \delta$[SNC](24) + *o*[NH](16) + τ[NCNC](19)
Form IV		
	24	Lattice
	29	Lattice
29	35	τ[SNCN](29) + $\tau[\varphi_3](57)$
39	40	$\tau[\varphi_1](27) + \tau[\varphi_2](36) + \tau$[NCNC](10) + $\tau[\varphi_3](13)$
58	51	$\tau[\varphi_1](69) + \tau$[NCNC](13)
64	58	Ph[*11b*](14) + τ[NCNC](64)
75	75	$\tau[\varphi_4](28) + \tau$[SNCN](71)
92	86	$\tau[\varphi_4](35) + \tau$[SNCN](27)
106	99	Ph[*11b*](12) + τ[NCNC](17) + $\tau[\varphi_2](37)$ + $\tau[\varphi_4](11)$
137	141	$\tau[\varphi_2](33) + \delta$[CSN](36) + *o*[NH](12)

[a] Types of vibration: ν, stretching; δ, deformation; τ, torsion; *o*, out of plane bending.
[b] Proposed assignment based on the PED for vibrational normal modes. Torsions are labeled according to Fig. 1. The six-membered aromatic ring (Ph) modes are labeled following the Wilson's notation.[55]

observations are in good agreement with the previously reported structural and spectroscopic data.[29]

In order to obtain further information from the measured spectra, some data treatment analysis must be applied. The traditional procedure is based on uni- or bivariate approaches, such as the one used in Ref. [29]. However, several nonlinear processes could be involved in solid-state transformations, which make specific peaks used for identification not well defined. This problem could be overcome using multivariate methods such as principal component analysis (PCA) and partial least-squares regression combined with methods of spectral preprocessing. Since in our case there is no need for a quantitative analysis, PCA is suitable to monitor the temperature evolution of our sample. PCA is a multivariate projection method that is used to extract and display systematic variation in a dataset. The results of the PCA calculations performed in the recorded spectra are presented in Fig. 8(c). Just one principal component (PC1) was necessary to describe the temperature evolution by considering the calculation in the 2800–3050 cm^{-1} spectral region. PC1 exhibits an anomaly around −50 °C, which can be associated to the beginning of the phase transition. This data treatment minimizes the artifacts due to spectra with highly overlapped bands and/or subtle spectral differences. However, this methodology fails to determine the extension of the phase coexistence region because a Raman

Journal of RAMAN SPECTROSCOPY

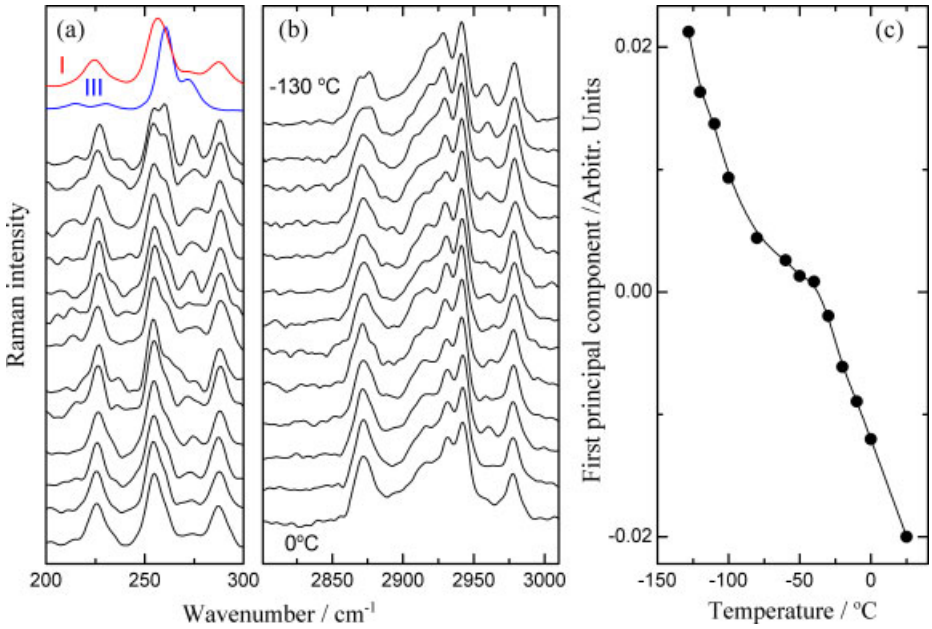

Figure 8. (a) and (b) Low-temperature Raman spectra of the form I of chlorpropamide. (c) Temperature dependence of the first principal component of the PCA treatment of the Raman spectra.

spectrum of the pure form of I′(ε′) is not available. Thus, the temperature evolution of PC1 above and below the anomaly could also be addressed to the thermal dependence of the Raman bands. In order to confirm the observations of Drebushchak *et al*.,[29] the room-temperature Raman spectra of forms I and III are included in Fig. 8(a). Remembering that the molecular conformation of form I′(ε′) is very close to that of form III, one may expect that bands associated with the orientation of the phenyl ring are at similar positions. As a consequence, it can be observed that the splitting of the 255 cm^{-1} band is due to the overlap of the corresponding bands of forms I′(ε′) and I, confirming the phase coexistence of these phases down to −130 °C.

Conclusions

The vibrational spectra of four polymorphs of chlorpropamide were investigated using Raman spectroscopy. In general, the FT-Raman spectra of polymorphs I, III, and IV exhibit only small differences, which do not allow a univocal identification by direct inspection. That is not the case of forms II and VI, which present significant wavenumber shifts characterizing these crystal forms. However, dispersive Raman spectra in the low wavenumber region show that lattice and skeleton deformation modes are very sensitive to the crystal form. The existence of a low-temperature phase transition in form I was also verified by Raman spectroscopy. It was also confirmed that forms I and I′ coexist over a wide temperature range. Theoretical calculations indicate that the optimized torsion angles agree well with the experimental twist values found for all the observed polymorphs. In fact, our calculations pointed out the relevance of the ethyl tail orientation, as observed in the form VI. It is also important to notice that no polymorphs exhibiting some specific energetic minima or their combinations have been reported yet, showing the possible existence of further crystal forms.

In summary, Raman spectroscopy was applied to the study of a polymorphic compound, emphasizing the key characteristic of this method. First, the spectroscopic fingerprints of all the polymorphs were obtained, allowing their identification in raw materials or formulated products. In particular, the capability of measuring molecular skeleton and lattice vibrations has played a very important role to study the conformational polymorphism of chlorpropamide. It is worthwhile to point out that the Raman spectroscopy is the only method capable of recording the complete vibrational spectra (5–4000 cm^{-1}) with the same experimental setup. Quantum mechanical calculations were carried out and the low wavenumber bands were successfully assigned to the normal modes of the molecule and crystal. In addition, the energy landscape was scanned and the observed polymorphs were correlated with the determined structures. Finally, the temperature dependence of the Raman spectra was recorded, depicting the capability of this technique for *in situ* monitoring kinetically induced processes.

Acknowledgements

The authors acknowledge financial support from CNPq-Prosul, FUNCAP, CAPES, FAPESP, CONICET, Ministerio de Ciencia y Tecnologia (Argentina) and Fundación Sauberan. S. L. Cuffini acknowledges financial support from Agencia Córdoba Ciencia. J. Ellena, A. P. Ayala, C.C.P. da Silva and J. Mendes Filho thank CNPq for research fellowships. S. B. Honorato thanks CAPES-PNPD for a research fellowship.

References

[1] B. Rodriguez-Spong, C. P. Price, A. Jayasankar, A. J. Matzger, N. Rodriguez-Hornedo, *Adv. Drug Deliv. Rev.* **2004**, *56*, 241.
[2] D. J. W. Grant, *Polymorphism in Pharmaceuticals*, Marcel Dekker: New York, **1999**, pp. 1.
[3] J. Bernstein, *Polymorphism in Molecular Crystals*, Oxford University Press: Oxford, **2002**.
[4] J. Haleblia, W. McCrone, *J. Pharm. Sci.* **1969**, *58*, 911.
[5] H. Ueda, N. Nambu, T. Nagai, *Chem. Pharm. Bull.* **1984**, *32*, 244.
[6] A. S. Raw, L. X. Yu, *Adv. Drug Deliv. Rev.* **2004**, *56*, 235.

[7] L. X. Yu, M. S. Furness, A. Raw, K. P. W. Outlaw, N. E. Nashed, E. Ramos, S. P. F. Miller, R. C. Adams, F. Fang, R. M. Patel, F. O. Holcombe, Y. Y. Chiu, A. S. Hussain, *Pharm. Res.* **2003**, *20*, 531.
[8] A. P. Ayala, *Vib. Spec.* **2007**, *45*, 112.
[9] J. Aaltonen, K. C. Gordon, C. J. Strachan, T. Rades, *Int. J. Pharm.* **2008**, *364*, 159.
[10] D. E. Bugay, *Adv. Drug Deliv. Rev.* **2001**, *48*, 43.
[11] G. Fini, *J. Raman Spectrosc.* **2004**, *35*, 335.
[12] A. Heinz, C. J. Strachan, K. C. Gordon, T. Rades, *J. Pharm. Pharmacol.* **2009**, *61*, 971.
[13] T. Vankeirsbilck, A. Vercauteren, W. Baeyens, G. Van der Weken, F. Verpoort, G. Vergote, J. P. Remon, *Trends Analyt. Chem.* **2002**, *21*, 869.
[14] C. S. Mizuno, A. G. Chittiboyina, T. W. Kurtz, H. A. Pershadsingh, M. A. Avery, *Curr. Med. Chem.* **2008**, *15*, 61.
[15] D. L. Simmons, R. J. Ranz, N. D. Gyanchandani, *Can. J. Pharm. Sci.* **1973**, *8*, 125.
[16] A. Burger, *Sci. Pharm.* **1975**, *43*, 152.
[17] A. Burger, *Pharm. Ind.* **1976**, *38*, 639.
[18] V. A. Drebushchak, T. N. Drebushchak, N. V. Chukanov, E. V. Boldyreva, *J. Therm. Anal. Calorim.* **2008**, *93*, 343.
[19] M. Otsuka, T. Matsumoto, N. Kaneniwa, *J. Pharm. Pharmacol.* **1989**, *41*, 665.
[20] M. Otsuka, Y. Matsuda, *Drug Dev. Ind. Pharm.* **1993**, *19*, 2241.
[21] W. J. Cao, S. Bates, G. E. Peck, P. L. D. Wildfong, Z. H. Qiu, K. R. Morris, *J. Pharm. Biomed. Anal.* **2002**, *30*, 111.
[22] E. V. Boldyreva, V. Dmitriev, B. C. Hancock, *Int. J. Pharm.* **2006**, *327*, 51.
[23] P. L. D. Wildfong, K. R. Morris, C. A. Anderson, S. M. Short, *J. Pharm. Sci.* **2007**, *96*, 1100.
[24] M. Koivisto, P. Heinanen, V. P. Tanninen, V. P. Lehto, *Pharm. Res.* **2006**, *23*, 813.
[25] T. Matsumoto, N. Kaneniwa, S. Higuchi, M. Otsuka, *J. Pharm. Pharmacol.* **1991**, *43*, 74.
[26] M. Otsuka, T. Matsumoto, S. Higuchi, K. Otsuka, N. Kaneniwa, *J. Pharm. Sci.* **1995**, *84*, 614.
[27] C. Vemavarapu, M. J. Mollan, T. E. Needham, *AAPS PharmSciTech* **2002**, *3*, 1.
[28] C. Koo, S. Cho, Y. Yeon, *Arch. Pharm. Res.* **1980**, *3*, 37.
[29] T. N. Drebushchak, Y. A. Chesalov, E. V. Boldyreva, *Acta Crystallogr. Sect. B Struct. Sci.* **2009**, *65*, 770.
[30] T. N. Drebushchak, N. V. Chukanov, E. V. Boldyreva, *Acta Crystallogr. Sect. C Cryst. Struct. Commun.* **2008**, *64*, O623.
[31] T. N. Drebushchak, N. V. Chukanov, E. V. Boldyreva, *Acta Crystallogr. Sect. C Cryst. Struct. Commun.* **2007**, *63*, O355.
[32] T. N. Drebushchak, N. V. Chukanov, E. V. Boldyreva, *Acta Crystallogr. Sect. E Struct. Rep.* **2006**, *62*, O4393.
[33] S. C. Perez, L. Cerioni, A. E. Wolfenson, S. Faudone, S. L. Cuffini, *Int. J. Pharm.* **2005**, *298*, 143.
[34] S. S. Al-Saieq, G. S. Riley, *Pharm. Acta Helv.* **1982**, *57*, 8.
[35] S. D. Yeo, M. S. Kim, J. C. Lee, *J. Supercrit. Fluids* **2003**, *25*, 143.
[36] Y. A. Chesalov, V. P. Baltakhinov, T. N. Drebushchak, E. V. Boldyreva, N. V. Chukanov, V. A. Drebushchak, *J. Mol. Struct.* **2008**, *891*, 75.
[37] A. M. Tudor, C. D. Melia, M. C. Davies, *J. Pharm. Pharmacol.* **1991**, *43*, 34.
[38] M. M. De Villiers, D. E. Wurster, *Acta Pharm.* **1999**, *49*, 79.
[39] A. M. Tudor, S. J. Church, P. J. Hendra, M. C. Davies, C. D. Melia, *Pharm. Res.* **1993**, *10*, 1772.
[40] J. J. McKinnon, M. A. Spackman, A. S. Mitchell, *Acta Crystallogr. Sect. B Struct. Sci.* **2004**, *60*, 627.
[41] M. J. Frisch, G. W. Trucks, H. B. Schlegel, G. E. Scuseria, M. A. Robb, J. R. Cheeseman, J. A. Montgomery, Jr., T. Vreven, K. N. Kudin, J. C. Burant, J. M. Millam, S. S. Iyengar, J. Tomasi, V. Barone, B. Mennucci, M. Cossi, G. Scalmani, N. Rega, G. A. Petersson, H. Nakatsuji, M. Hada, M. Ehara, K. Toyota, R. Fukuda, J. Hasegawa, M. Ishida, T. Nakajima, Y. Honda, O. Kitao, H. Nakai, M. Klene, X. Li, J. E. Knox, H. P. Hratchian, J. B. Cross, C. Adamo, J. Jaramillo, R. Gomperts, R. E. Stratmann, O. Yazyev, A. J. Austin, R. Cammi, C. Pomelli, J. W. Ochterski, P. Y. Ayala, K. Morokuma, G. A. Voth, P. Salvador, J. J. Dannenberg, V. G. Zakrzewski, S. Dapprich, A. D. Daniels, M. C. Strain, O. Farkas, D. K. Malick, A. D. Rabuck, K. Raghavachari, J. B. Foresman, J. V. Ortiz, Q. Cui, A. G. Baboul, S. Clifford, J. Cioslowski, B. B. Stefanov, G. Liu, A. Liashenko, P. Piskorz, I. Komaromi, R. L. Martin, D. J. Fox, T. Keith, M. A. Al-Laham, C. Y. Peng, A. Nanayakkara, M. Challacombe, P. M. W. Gill, B. Johnson, W. Chen, M. W. Wong, C. Gonzalez, J. A. Pople, *Gaussian 03, Revision C.02.*, Gaussian Inc.: Wallingford, CT, **2004**.
[42] R. G. Parr, W. Yang, *Density Functional Theory of Atoms and Molecules*, Oxford University Press: New York, **1989**.
[43] C. T. Lee, W. T. Yang, R. G. Parr, *Phys. Rev. [Sect.] B* **1988**, *37*, 785.
[44] A. D. Becke, *J. Chem. Phys.* **1993**, *98*, 5648.
[45] P. L. Polavarapu, *J. Phys. Chem.* **1990**, *94*, 8106.
[46] S. Mishra, D. Chaturvedi, P. Tandon, V. P. Gupta, A. P. Ayala, S. B. Honorato, H. W. Siesler, *J. Phys. Chem. A* **2009**, *113*, 273.
[47] J. M. L. Martin, C. Van Alsenoy, *GAR2PED Program*. University of Antwerp: Antwerpen, Belgium, **1995**.
[48] P. Pulay, G. Fogarasi, F. Pang, J. E. Boggs, *J. Am. Chem. Soc.* **1979**, *101*, 2550.
[49] D. E. Braun, T. Gelbrich, V. Kahlenberg, R. Tessadri, J. Wieser, U. J. Griesser, *J. Pharm. Sci.* **2009**, *98*, 2010.
[50] N. Zencirci, T. Gelbrich, V. Kahlenberg, U. J. Griesser, *Cryst. Growth Des.* **2009**, *9*, 3444.
[51] A. P. Ayala, H. W. Siesler, R. Boese, G. G. Hoffmann, G. I. Polla, D. R. Vega, *Int. J. Pharm.* **2006**, *326*, 69.
[52] A. P. Ayala, H. W. Siesler, S. L. Cuffini, *J. Raman Spectrosc.* **2008**, *39*, 1150.
[53] E. V. Brusau, G. E. Cami, G. E. Narda, S. L. Cuffini, A. P. Ayala, J. Ellena, *J. Pharm. Sci.* **2008**, *97*, 542.
[54] M. de Veij, P. Vandenabeele, T. De Beer, J. P. Remonc, L. Moens, *J. Raman Spectrosc.* **2009**, *40*, 297.
[55] G. Varsanyi, *Vibrational Spectra of Benzene Derivatives*, Academic Press: New York, **1969**.
[56] A. P. Ayala, H. W. Siesler, S. M. S. V. Wardell, N. Boechat, V. Dabbene, S. L. Cuffini, *J. Mol. Struct.* **2007**, *828*, 201.
[57] A. Srivastava, S. Mishra, P. Tandon, S. Patel, A. P. Ayala, A. K. Bansal, H. W. Siesler, *J. Mol. Struct.* **2010**, *964*, 3.
[58] F. T. Martins, A. P. Ayala, W. Porcal, H. Cerecetto, M. González, J. Ellena, *Mol. Divers.* **2010**, *14*, 643.
[59] G. I. Polla, D. R. Vega, H. Lanza, D. G. Tombari, R. Baggio, A. P. Ayala, J. Mendes, D. Fernandez, G. Leyva, G. Dartayet, *Int. J. Pharm.* **2005**, *301*, 33.
[60] H. Wikstrom, C. Kakidas, L. S. Taylor, *J. Pharm. Biomed. Anal.* **2009**, *49*, 247.
[61] M. Sardo, A. M. Amado, P. J. A. Ribeiro-Claro, *J. Raman Spectrosc.* **2008**, *39*, 1915.
[62] G. Fevotte, *Chem. Eng. Res. Des.* **2007**, *85*, 906.